

Pressure-temperature phase diagram of UPd_2Si_2 and UNi_2Si_2

G. Quirion and F. S. Razavi

Department of Physics, Brock University, St. Catharines, Ontario, Canada L2S 3A1

M. L. Plumer*

Centre de Recherche en Physique du Solide, Département de Physique, Université de Sherbrooke, Sherbrooke, Québec, Canada J1K 2R1

J. D. Garrett

Brockhouse Institute for Materials Research, McMaster University, Hamilton, Ontario, Canada L8S 4M1

(Received 19 June 1997; revised manuscript received 26 September 1997)

It is well established that the ternary intermetallic family of compounds UT_2Si_2 , where T denotes a transition metal, shows a rich variety of electronic and magnetic ground-state properties. In order to better understand the magnetic properties of these materials, we have investigated the behavior of the electrical resistivity of UNi_2Si_2 and UPd_2Si_2 as a function of temperature and pressure. In the case of UNi_2Si_2 , the proposed pressure-temperature phase diagram is very similar to its magnetic-field-temperature phase diagram. The pressure-temperature phase diagram obtained for both compounds is also compared to predictions made using a mean-field Landau-type analysis. [S0163-1829(98)02809-4]

I. INTRODUCTION

The intermetallic compounds UT_2Si_2 , where T stands for a transition metal, have been widely investigated in the past years. Most of these materials, which crystallize in the body-centered tetragonal (bct) ThCr_2Si_2 structure, have a strong c -axis magnetic anisotropy, as well as a long-range Ruderman-Kittel-Kasuya-Yosida (RKKY) interaction. As a result of the relative strength of these two interactions, a rich variety of electronic and magnetic ground-state properties are possible.¹ Among this family of compounds, the heavy-fermion metal URu_2Si_2 has attracted a considerable amount of attention mainly because of the unusual coexistence of superconductivity and antiferromagnetism at low temperatures.²⁻⁴ Consequently, less attention has been directed toward magnetically ordered systems in this family such as UNi_2Si_2 and UPd_2Si_2 . These materials are, however, interesting in their own right. Even if both compounds are very similar in many aspects, the observed magnetic ground states are quite different.^{5,6} For instance, it has been demonstrated that the axial next-nearest-neighbor Ising (ANNNI) model and its extensions can adequately predict the sequence of magnetic phases observed in UPd_2Si_2 ;⁷ however, for UNi_2Si_2 , a more complex model is required.⁸ Consequently, in order to better understand the unusual physical properties of UNi_2Si_2 , we compare in this paper the behavior of the electrical resistivity of UNi_2Si_2 and UPd_2Si_2 as a function of temperature and pressure. The pressure-temperature phase diagram obtained for both compounds is also compared to predictions made using a mean-field Landau-type analysis.

II. EXPERIMENT

All measurements were done on single crystals grown by a modified triple-arc Czochralski method.⁹ Hydrostatic pressure was generated using a cylindrical Cu-Be piston device with a 1:1 mixture of 3-methyl-1-butanol and

2-methylbutane acting as the pressure-transmitting medium. The pressure inside the cell was monitored at room temperature by measuring the resistivity change of a lead sample mounted next to the sample. During the cooling process, a pressure loss of about 2 kbar occurs, which must be accounted for in the data analysis. The dc electrical resistivity of UPd_2Si_2 and UNi_2Si_2 was then measured by a standard four-probe method between 4.2 and 300 K at pressures up to about 14 kbar. The measurements for UPd_2Si_2 have been obtained with the direction of the electric current perpendicular to the c axis (ρ_\perp), while for UNi_2Si_2 the current was parallel to the c axis (ρ_\parallel).

III. RESULTS AND DISCUSSION

Figure 1 shows the temperature dependence of the resistivity UPd_2Si_2 measured at different pressures. At 1 bar, the overall temperature dependence displays the same behavior as obtained previously by other groups^{10,11} for ρ_\perp . We clearly observe two distinct breaks that coincide with the expected phase transitions for UPd_2Si_2 at ambient pressure, one at 108 K and the other at 136 K. The magnetic neutron scattering measurement⁵ indicates that the magnetic moments, which are localized on the uranium atoms, form an antiferromagnetic ($\langle 1 \rangle$) structure at low temperatures. Between 108 and 136 K, the system takes on an incommensurate (IC) longitudinal spin-density-wave structure that runs along the c axis. In both magnetic ordered phases, the localized spin on the uranium atoms points along the c axis of the crystal. Finally, at 136 K the IC structure transforms into the usual high-temperature paramagnetic (P) state. Furthermore, when the derivative of the resistivity (not shown here) is carefully examined, an additional small anomaly is observed at 38 K. The existence of a phase transition at 40 K has previously been reported in neutron scattering studies performed on polycrystalline samples.¹² However, more recent neutron scattering measurements⁵ on a single crystal have

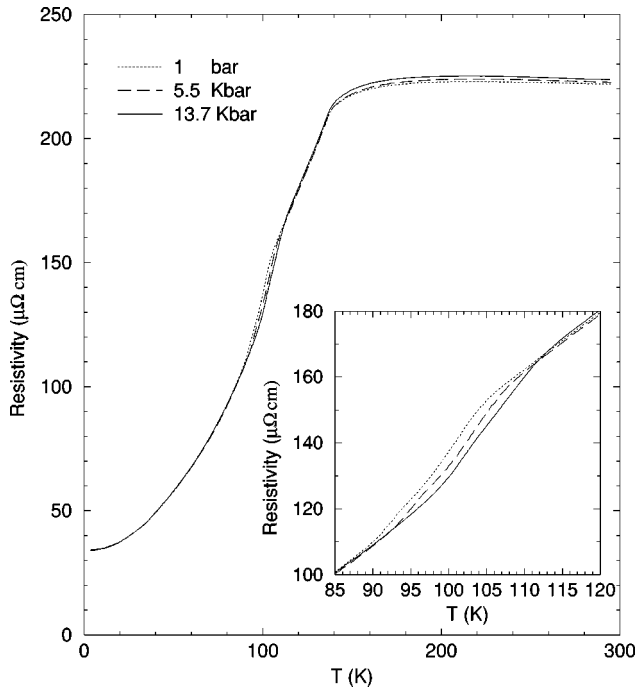


FIG. 1. Temperature dependence of the resistivity (ρ_{\perp}) of UPd_2Si_2 with the current perpendicular to the c axis for pressures $P=1$ bar, 5.5 kbar, and 13.7 kbar. The inset magnifies the data to show more clearly the effect of pressure on the phase transition at 108 K.

ruled out that possibility. Therefore, considering that the resistivity change at 38 K is hardly noticeable, we attribute the additional anomaly to the presence of a very small component of some secondary phase in the sample. This conclusion is further supported by the fact that pressure has no effect on this low-temperature anomaly. Finally, as shown in the inset of Fig. 1, we see more clearly that the $\langle 1 \rangle$ -IC phase transition at 108 K is displaced with the application of pressure to a higher temperature at a rate of $+0.58$ K/kbar. However, the IC-P phase transition remains unaffected.

The observed sequence of magnetically ordered phases for UNi_2Si_2 (Ref. 13) is different from what has been described above for UPd_2Si_2 .^{11,14} As shown by the neutron diffraction investigation,^{6,15} UNi_2Si_2 has three magnetically ordered phases, in all of which the magnetic moments of the uranium atoms are also aligned along the c axis. The low-temperature phase ($T < 53$ K) can be interpreted as a commensurate longitudinal spin-density wave with $Q=(0,0,\frac{2}{3})$ that coexists with ferromagnetism (CLSDW+ferro). This magnetic structure can also be regarded as a phase where two-thirds of the spins point along the positive z direction and one-third along the negative z direction; this phase is also known as the $\langle 12 \rangle$ phase. In the intermediate-temperature phase, which extends from 53 K up to 103 K, the system is a simple body-centered antiferromagnet ($\langle 1 \rangle$). The last ordered phase between 103 K and 123 K is characterized by an incommensurate longitudinal spin-density wave (IC) with a temperature-dependent wave vector q less than $\frac{3}{4}$. Above 123 K the system is paramagnetic (P). Therefore, the sequence of phases observed with increasing temperature can be summarized as follows: $\langle 12 \rangle \rightarrow \langle 1 \rangle \rightarrow \text{IC} \rightarrow P$. As discussed in Ref. 8, it is generally very unusual to

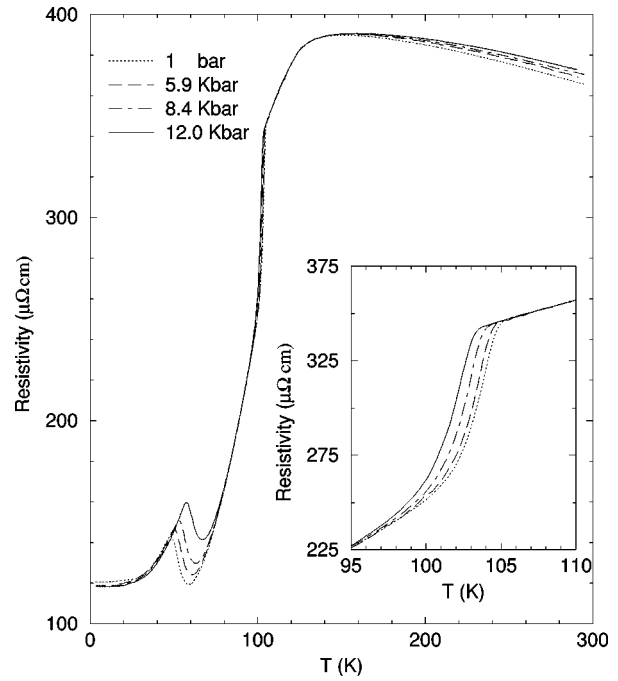


FIG. 2. Temperature dependence of the resistivity (ρ_{\parallel}) of UNi_2Si_2 with the current parallel to the c axis for pressures $P=1$ bar, 5.9 kbar, 8.4 kbar, and 12.0 kbar. The inset magnifies the data to show more clearly the effect of pressure on the phase transition at 103 K.

observe a temperature-induced transition to a shorter-period modulated structure of *any type*. All of these phase transitions can be observed in the temperature dependence of the c -axis resistivity shown in Fig. 2. As in the case for UPd_2Si_2 , we note that only the phase transition at 124 K, which also corresponds to a second-order phase transition from IC to P, is unaffected by pressure. Moreover, we observe a moderate shift of the $\langle 1 \rangle$ -IC phase boundary at 103 K. In contrast with UPd_2Si_2 , for UNi_2Si_2 the critical temperature is reduced by pressure at a rate of -0.14 K/kbar. Finally, we also observe a significant pressure dependence on the $\langle 12 \rangle$ - $\langle 1 \rangle$ phase transition at 53 K of $+0.77$ K/kbar.

The temperature dependence of the resistivity for UNi_2Si_2 below 53 K (in the $\langle 12 \rangle$ phase) is comparable to what has been obtained for isostructural compounds like URu_2Si_2 (Ref. 16) and UNi_2Ge_2 .¹⁷ In all these compounds, the sudden increase of the resistivity at the phase boundary has been attributed to the opening of a gap on part of the Fermi surface. This anisotropic gap is induced by the commensurate modulation of the spin density wave (SDW) along the c axis. One consequence of this gap is to reduce the effective number of conduction electrons which explains the increase in the resistivity just below the transition temperature. However, for UNi_2Si_2 the jump in the resistivity is not as sharp as what is observed, for example, in URu_2Si_2 and UNi_2Ge_2 . That might indicate rather that a pseudogap is opened in UNi_2Si_2 . As we increase pressure, this phase transition moves rapidly to higher temperatures while the amplitude of the resistivity jump decreases slightly. This trend is again consistent with the results obtained for URu_2Si_2 .^{18,19} Moreover, the temperature dependence of the resistivity in the $\langle 12 \rangle$ phase is well described by a gapped spin-wave model plus a T^2 term associated with the electron-electron interac-

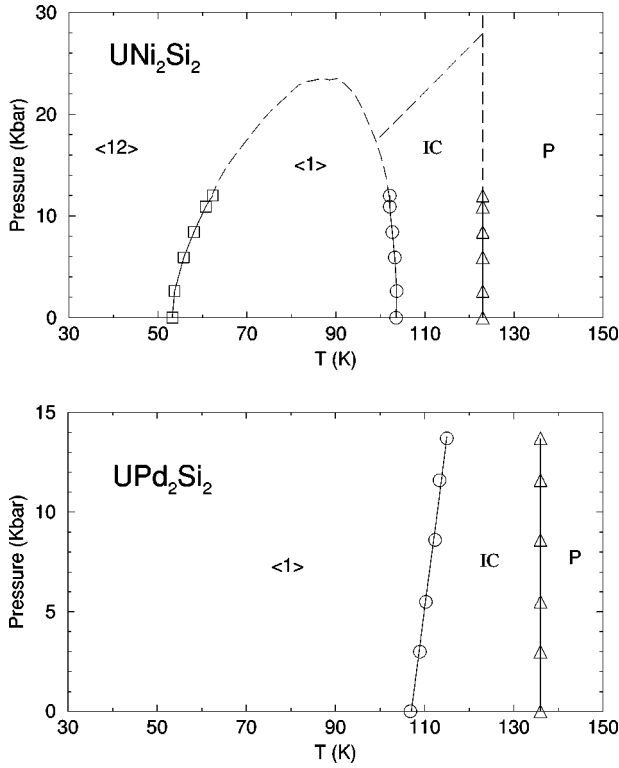


FIG. 3. Pressure-temperature magnetic phase diagram of UPd_2Si_2 and UNi_2Si_2 .

tion. The resistivity between 4.2 K and 45 K can thus be fitted to the expression

$$\rho(T) = \rho_0 + AT^2 + BT(1 + 2T/\Delta)e^{-\Delta/T},$$

where ρ_0 is the residual resistivity, Δ is the amplitude of the energy gap in the spin-wave (magnon) structure which is the dominant scattering mechanism for electrons, and A and B are constants. Fitting $\rho(T)$ to this expression, we obtain, for UNi_2Si_2 , $\rho_0 = 118.6 \mu\Omega \text{ cm}$, $A = 0.99 \times 10^{-3} \mu\Omega \text{ cm K}^{-2}$, $B = 2.32 \mu\Omega \text{ cm K}^{-1}$, and $\Delta = 109 \text{ K}$. These values are comparable with those obtained by Ning *et al.*²⁰ Note that the amplitude of the gap is pressure independent. This is different from what has been observed for URu_2Si_2 .^{18,19} In that case the spin-wave gap does change significantly under pressure.

In Fig. 3, we present the pressure-temperature phase diagram of UNi_2Si_2 and UPd_2Si_2 . These phase diagrams have been deduced from the anomalies observed in the resistivity measurements. In the case of UNi_2Si_2 , although our pressure experiments do not extend above 12 kbar to reveal the upper field boundary, we have also included additional proposed boundary lines based mainly on its similarity with the corresponding magnetic-field-temperature phase diagram.¹³ Moreover, as we will now show, many features of both pressure-temperature phase diagrams can also be explained using a Landau-type approach.

Inspired by the success of a Landau-type analysis of the magnetic-field-temperature phase diagram of UPd_2Si_2 ,^{7,8,11,14} we now consider the effect of pressure on the magnetic ordering process in the class of UT_2X_2 compounds. The magnetic interactions are well described by a Heisenberg-type Hamiltonian of the form

$$\mathcal{H} = -\frac{1}{2} \sum_{ij} J(\mathbf{r}_i - \mathbf{r}_j) \mathbf{s}(\mathbf{r}_i) \cdot \mathbf{s}(\mathbf{r}_j), \quad (1)$$

where the spin-density vector $\mathbf{s}(\mathbf{r}_i)$ is assumed to lie along the bct c axis ($\parallel \hat{\mathbf{z}}$) due to strong axial anisotropy. Due to the ferromagnetic in-plane interactions $J_0 < 0$, the problem effectively becomes that of frustration in one dimension due to the competition between first-, second-, and third-neighbor exchange interactions (J_1 , J_2 , and J_3), likely of the RKKY type in origin, along the c axis among planes separated by $c' = \frac{1}{2}c$. In the ANNNI-type model of Refs. 7 and 8, $J_1 < 0$ and $J_2 < 0$ are antiferromagnetic (AF), while $J_3 > 0$ is ferromagnetic. In addition to the incommensurate state (IC), only two commensurate phases appear for values of J_2/J_1 that are not too large. These are the period-2 AF ($\langle 1 \rangle$) and period-3 ($\langle 12 \rangle$) phases. As a function of temperature, four possible sequences of phases may occur within the mean-field approximation depending on the value of J_2/J_1 (with J_3 set to a small value). One of these sequences is $\langle 1 \rangle$ -IC- P , as observed in UPd_2Si_2 . As discussed at length in Ref. 8, the sequence $\langle 12 \rangle$ - $\langle 1 \rangle$ -IC- P found in UNi_2Si_2 cannot be reproduced by this simple model. Such a low-temperature transition ($\langle 12 \rangle$ - $\langle 1 \rangle$) requires not only the addition of a bi-quadratic exchange interaction, but occurs only then as a consequence of effects due to critical fluctuations not accounted for in the present approach.

Some essential features of the magnetic phase diagram are, however, captured by the Landau approach. The most significant is the increasing stability of the period-3 state with the application of a magnetic field along the c axis. In the presence of an applied magnetic field, the spin density is written as

$$\mathbf{s}(z) = \mathbf{m} + \mathbf{S}e^{iQz} + \mathbf{S}^*e^{-iQz}, \quad (2)$$

where \mathbf{m} is the uniform component due to the applied field, \mathbf{S} is the complex polarization vector, and Q is the wave vector. For $\mathbf{m} \parallel \mathbf{S}$, a term of the form $m(S^3 + \text{c.c.})\Delta_{3Q,G}$ occurs, where G is a reciprocal lattice vector along the c axis. Thus, if $3Q = G$, as in the period-3 phase, an incipient uniform component ($m \sim H$) is induced. It is the coupling of m to the applied magnetic field which serves to enhance the stability of this state and significantly affects the nature of the phase diagram. In the case of UPd_2Si_2 , the $\langle 12 \rangle$ phase appears only at ‘‘high’’ field strengths.

An analogous term, e.g., PS^3 , cannot occur in the case of applied pressure (or uniaxial stress). This is due to the fact that it is third order in S and thus requires a coupling field (e.g., m) which changes sign under time-reversal symmetry, as does S itself. However, pressure may have a significant effect since, as shown below, it can alter the relationship between exchange interactions J_n and thus disturb the delicate balance of frustration which gives rise to the variety of magnetic phases observed in the UT_2X_2 compounds.

It is assumed here that the free energy can be written as the sum of three terms,²¹

$$F = F_s + F_e + F_{es}, \quad (3)$$

where F_s is the purely magnetic contribution (fully discussed in Ref. 7), F_e is the elastic energy,

$$F_e = \frac{1}{2} \sum_{ij} C_{ij} e_i e_j, \quad (4)$$

where $i, j = 1-6$ in the Voigt notation and e_i are the components of the strain tensor, and finally F_{es} represents magnetoelastic coupling. To lowest order $\sim e s^2$, this latter term has only one contribution for systems with tetragonal symmetry where $s \parallel \hat{z}$:

$$F_{es} = \frac{1}{2V} \int dz dz' K(z-z') e_3 s(z) s(z'). \quad (5)$$

The structure of this term is identical to the second-order contribution to F_s discussed in Ref. 7 (since e_3 is assumed to be constant). Using the above expression for the spin density thus yields

$$F_{es} = \frac{1}{2} k_0 m^2 + k_q |S|^2 + \frac{1}{2} k_q [S^2 + \text{c.c.}] \Delta_{2Q,G}, \quad (6)$$

where k_q is the Fourier transform of the magnetoelastic coupling ($q = cQ/2$),

$$k_q = 4k_0 + 2[k_1 \cos q + k_2 \cos(2q) + k_3 \cos(3q)]. \quad (7)$$

Note that $2Q = G$ only in the case of the period-2 phase $\langle 1 \rangle$. This expression is similar to the Fourier transform of the exchange integral J_q of Ref. 7 with k_0 being the in-plane contribution and the other terms corresponding to first-, second-, and third-neighbor interactions in the z direction. Thus, second-order terms in the full free energy now appear with a renormalized exchange interaction $J_n \rightarrow J_n + e_3 k_n$. This formulation makes clear that magnetoelastic coupling accounts for the variation of the exchange interaction with ionic separation²² $J(r) = J(r_0) + (r - r_0) \cdot \nabla J(r_0) + \dots$.

Following Ref. 23, the equilibrium properties are determined by minimization of the Gibbs free energy $G = F - \sum_i \sigma_i e_i$, where σ_i is the applied stress tensor. In the case of applied hydrostatic pressure P , $\sigma_i = -P$ for $i = 1, 2, 3$, and the other components are zero. Minimizing G with respect to e_i yields elastic contributions of the form

$$G_{el} = -\beta P [k_0 m^2 + 2k_q |S|^2 + k_q (S^2 + \text{c.c.}) \Delta_{2Q,G}] - \frac{1}{2} s_{33} [k_0 m^2 + 2k_q |S|^2 + k_q (S^2 + \text{c.c.}) \Delta_{2Q,G}]^2, \quad (8)$$

where $\beta = 2s_{13} + s_{33}$ and s_{ij} is the compliance tensor (the inverse of C_{ij}). The complete Gibbs free energy given by $G = F_s + G_{el}$ thus has a form identical to F considered in Ref. 7. Here, the exchange interactions are renormalized by the applied pressure, $J_n \rightarrow J_n + \beta P k_n$, and in addition, some of the fourth-order coefficients are modified by the latter contribution to G_{el} .

As discussed in Refs. 7 and 8, it appears that at least UNi_2Si_2 and UPd_2Si_2 have values of J_2/J_1 which are close to 0.35 where phases $\langle 1 \rangle$ and $\langle 12 \rangle$ are degenerate at zero temperature. There is thus the possibility for a magnetic field-, pressure-, and temperature-induced frustration leading to phase transitions. Since only relatively small changes in the effective exchange interactions can induce a variety of transitions among the three order phases (IC included), and since the signs and strengths of the magnetoelastic coupling

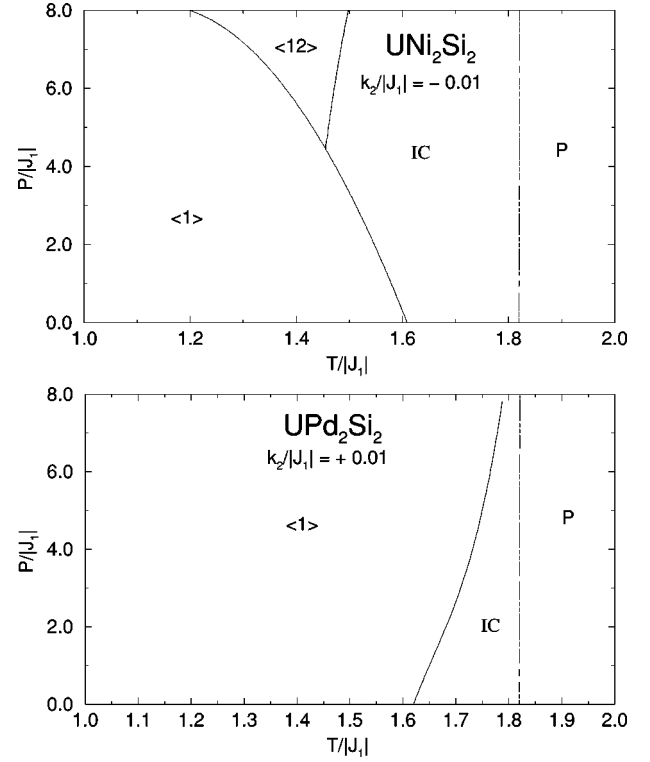


FIG. 4. Magnetic phase diagram with exchange parameters $J_0 = 1$, $J_1 = -1$, $J_2 = -0.30$, and $J_3 = 0.03$ and $k_2/|J_1| = +0.01$ for UPd_2Si_2 and $k_2/|J_1| = -0.01$ for UNi_2Si_2 . Solid and dashed curves represent first-order and continuous transitions, respectively. The AF phase is labeled as $\langle 1 \rangle$.

constants k_n are unknown, there are a large number of phase diagram types which could occur as a function of pressure and temperature.

For the purpose of illustration, only two cases are considered here. Values for the exchange interactions used in Ref. 7 to model UPd_2Si_2 are adopted for this study: $J_0 = 1$, $J_1 = -1$, $J_2 = -0.30$, and $J_3 = 0.03$. With these values, gross features of the magnetic-field-temperature phase diagram are correctly reproduced.^{11,14} For simplicity, only the effects of a nonzero second-neighbor magnetoelastic coupling constant k_2 are considered. Values of this constant, as well as the pressure P , are normalized to $|J_1|$. Also, for simplicity, we set $\beta \equiv 1$, $s_{33} \equiv 1$, and consider values $k_2/|J_1| = \pm 0.01$.

The results shown in Fig. 4 demonstrate that for a positive $k_2/|J_1| = +0.01$ ratio, the effect of pressure is to increase the value of the second-neighbor exchange interaction (making J_2 less negative), thereby increasing the region of stability of the period-2 phase $\langle 1 \rangle$. In addition, the IC-P boundary is hardly affected. These qualitative features are also found in the experimental results for UPd_2Si_2 (see Fig. 3), although there is no particular reason why only k_2 should be nonzero in this compound. In contrast, Fig. 4 shows that by simply changing the sign of $k_2/|J_1| = -0.01$, the effect of pressure is to decrease the value of J_2 so that the $\langle 1 \rangle$ phase is less stable and the period-3 $\langle 12 \rangle$ state may appear at high enough pressure, as in the case of an applied magnetic field (although for completely different reasons). Therefore, this approach does adequately reproduce the observed pressure dependence of the $\langle 1 \rangle$ -IC phase boundary in both samples (see Fig. 3). However, in the case of UNi_2Si_2 it has been shown

that this approach is incompatible with the observed $\langle 12 \rangle$ magnetic ground state. Nevertheless, it remains valid for the description of the other boundaries at higher temperatures. Therefore, the results of Fig. 4 support the proposed pressure-temperature phase diagram for UNi_2Si_2 presented in Fig. 3.

Finally, we note that an additional effect of magnetoelastic coupling is to produce an effective fourth-order (in S) coefficient that is wave vector dependent. This leads to a temperature (and pressure) dependence of the spin-density-wave vector Q in the IC phase.²²

In summary, we have shown how pressure may alter the relationship between exchange interactions J_n and thus disturb the delicate balance of frustration which gives rise to the observed pressure-temperature phase diagram for the UPd_2Si_2 and UNi_2Si_2 . A simple model based on a Landau-

type free energy seems to capture the essential features of the magnetic-field–pressure–temperature phase diagrams of the UPd_2Si_2 and UNi_2Si_2 compounds at high temperatures. It is clear that, in order to prove that the proposed pressure-temperature phase diagram is adequate, measurements at higher pressures are needed. Moreover, more work is also needed in order to clarify the fundamental difference between these two systems.

ACKNOWLEDGMENTS

This work was supported by grants from the Natural Sciences and Engineering Research Council of Canada (NSERC). We are also grateful to Professor W.R. Datars for providing us with samples of these compounds.

-
- *Present address: Seagate Recording Heads, 7801 Computer Ave. So., Bloomington, MN 55435-5489.
- ¹T.T.M. Palstra, A.A. Menovsky, G.J. Nieuwenhuys, and J.A. Mydosh, *J. Magn. Magn. Mater.* **54-57**, 435 (1986).
 - ²W. Schlabit, J. Baumann, B. Pollit, U. Rauchschwalbe, H.M. Mayer, U. Ahlheim, and C.D. Bredl, *Z. Phys. B* **62**, 171 (1986).
 - ³T.T.M. Palstra, A.A. Menovsky, J. Van Den Berg, A.J. Dirkmaat, P.H. Kes, G.J. Nieuwenhuys, and J.A. Mydosh, *Phys. Rev. Lett.* **55**, 2727 (1985).
 - ⁴C. Broholm, J.K. Kjems, W.J.L. Buyers, P. Matthews, T.T.M. Palstra, A.A. Menovsky, and J.A. Mydosh, *Phys. Rev. Lett.* **58**, 1467 (1987).
 - ⁵B. Shemirani, H. Lin, M.F. Collins, C.V. Stager, J.D. Garrett, and W.J.L. Buyers, *Phys. Rev. B* **47**, 8672 (1993).
 - ⁶L. Rebersky, H. Lin, M.F. Collins, J.D. Garrett, W.J.L. Buyers, M.W. McElfresh, and M.S. Torikachvili, *J. Appl. Phys.* **69**, 4807 (1991).
 - ⁷M.L. Plumer, *Phys. Rev. B* **50**, 13 003 (1994).
 - ⁸A. Mailhot, M.L. Plumer, A. Caillé, and P. Azaria, *Phys. Rev. B* **45**, 10 399 (1992).
 - ⁹A.LeR. Dawson, W.R. Datars, J.D. Garrett, and F.S. Razavi, *J. Phys.: Condens. Matter* **1**, 6817 (1989).
 - ¹⁰M. Barati, W.R. Datars, T.R. Chien, C.V. Stager, and J.D. Garrett, *Phys. Rev. B* **48**, 16 926 (1993).
 - ¹¹T. Honma, H. Amitsuka, T. Sakakibara, K. Sugiyama, and M. Date, *Physica B* **186-8**, 684 (1993).
 - ¹²H. Ptasiwicz-Bak, J. Leciejewicz, and A. Zygmunt, *J. Phys. F* **11**, 1225 (1981).
 - ¹³S. W. Zochowski, S.A. Creeger, and M.F. Collins, *J. Magn. Magn. Mater.* **140-144**, 1399 (1995).
 - ¹⁴M.F. Collins, B. Shemirani, C.V. Stager, J.D. Garrett, H. Lin, W.J.L. Buyers, and Z. Tun, *Phys. Rev. B* **48**, 16 500 (1993).
 - ¹⁵H. Lin, L. Rebersky, M.F. Collins, J.D. Garrett, and W.J.L. Buyers, *Phys. Rev. B* **43**, 13 232 (1991).
 - ¹⁶T.T.M. Palstra, A.A. Menovsky, and J.A. Mydosh, *Phys. Rev. B* **33**, 6527 (1986).
 - ¹⁷Y.B. Ning, J.D. Garrett, C.V. Stager, and W.R. Datars, *Phys. Rev. B* **46**, 8201 (1992).
 - ¹⁸M. Ido, Y. Segawa, H. Amitsuka, and Y. Miyako, *J. Phys. Soc. Jpn.* **62**, 2962 (1993).
 - ¹⁹Y. Uwatoko, K. Iki, G. Oomi, Y. Onuki, and T. Komatsubara, *Physica B* **177**, 147 (1992).
 - ²⁰Y.B. Ning, J.D. Garrett, and W.R. Datars, *J. Phys.: Condens. Matter* **4**, 9995 (1992).
 - ²¹M.L. Plumer and A. Caillé, *Phys. Rev. B* **37**, 7712 (1988).
 - ²²M.L. Plumer, *Phys. Rev. B* **44**, 12 376 (1991).
 - ²³M.B. Walker, *Phys. Rev. B* **22**, 1338 (1980).